Bull. Mater. Sci., Vol. 38, No. 5, September 2015, pp. 1213–1221. © Indian Academy of Sciences.

Temperature-dependent ionic conductivity and transport properties of $LiClO_4$-doped PVA/modified cellulose composites

SUNIL G RATHOD[1], R F BHAJANTRI[2,*], V RAVINDRACHARY[1], P K PUJARI[3], G K NAGARAJA[4], JAGADISH NAIK[1], VIDYASHREE HEBBAR[2] and H CHANDRAPPA[2]

[1]Department of Physics, Mangalore University, Mangalagangotri 574 199, India
[2]Department of Physics, Karnatak University, Dharwad 580 003, India
[3]Radiochemistry Division, Bhabha Atomic Research Centre, Trombay, Mumbai 400 085, India
[4]Department of Chemistry, Mangalore University, Mangalagangotri 574 199, India

MS received 27 January 2015; accepted 18 May 2015

Abstract. **This paper presents the investigation on physicochemical properties and ionic conductivity of $LiClO_4$-doped poly(vinyl alcohol) (PVA)/modified cellulose composites. The percolative behaviour of $LiClO_4$ with dc conductivity (σ_{dc}) for different $LiClO_4$ weight fractions (p) related to transport dimensionality was also focused. The highest ionic conductivity of 9.79×10^{-6} S cm^{-1} was observed for 20 wt% $LiClO_4$ doping level at room temperature. The activation energies (E_g) were estimated using temperature-dependent conductivity, which follows the Arrhenius and Vogel–Tammann–Fulcher (VTF) relation. The dynamic fragility (f) and activation energy (E_g) *vs.* T_g of polymer composites using equivalence of the both Williams–Landel–Ferry (WLF) and VTF equations were also correlated. Transport properties such as travel time of ions between sites (τ_0), mobility (μ), diffusion coefficient (D) and number of transitions per unit time $P(E)$ for normal cationic (Li^+) hopping process of $LiClO_4$-doped PVA/mCellulose composites have been investigated using the Rice and Roth model.**

Keywords. **Percolation; transport properties; VTF model; ionic conductivity; Williams–Landel–Ferry.**

1. Introduction

In recent years, the application of solid polymer-based composites have received great attention due to their flexible and renewable energy storage devices.[1,2] Also, these polymeric composites have potential applications in the low-cost manufacture of various electronic devices, such as inkjet, screen or gravure printing, organic field-effect transistors, flexible circuits, electric paper, sensors, etc. However, the use of these materials is limited by the achievable ionic conductivities at ambient temperature. Hence, considerable attention has been given to the study of basic ion transport properties and ion interactions involving these complexes.[3–5] It has been shown that the ionic conduction mainly coupled with the relaxation time for the segmental motion of the polymer matrix. This segmental motion plays an important role in the transport mechanism and also facilitates the ionic diffusion in the host polymer.[6]

Preparation of the polymer composite is to achieve the fast ionic diffusion, which depends on the glass transition temperatures (T_g) and co-ordinating side chains for the ionic transport. In this regard, most percolation models are based on the hypothesis that T_g in materials occur as a result of the percolation of slow, immobile domains through the system.[7–9] Hence, T_g has been the most thoroughly investigated property of the polymers and study on lowering of the T_g of polymers is to be paid much attention. Although decrease in T_g enhances the ionic conductivity and mobility of the carrier ions, doping the higher concentration of salts in the polymer matrix leads to decrease in the ionic mobility, which is caused by the suppression of the polymer dynamics, which is reflected in an increase in the T_g. Hence, the change in T_g along with high mobility can be obtained through an enhancement of the amorphous phase at higher doping of salt by altering the physical properties of the polymers.[10]

Polymer blending has already been established as an effective means for constructively altering the transport properties and T_g of the polymeric materials.[11,12] Blending of cellulose with poly(vinyl alcohol) (PVA) is favourable because both the polymers have polar substances with many hydroxyl groups in their chemical structure. These highly polar hydroxyl groups tend to form intermolecular and intramolecular hydrogen bonds

*Author for correspondence
(rfbhajantri@gmail.com, rfbhajantri@kud.ac.in)

between hydroxyl groups of cellulose and PVA promotes the localized stability in the polymer structure; subsequently enhancement in the transport properties can be expected.

The hydrophilic nature of the modified cellulose (mCellulose) and water-soluble PVA is a well-suited matrix to blend. When salt is doped into such polymer composites, the hydroxyl groups in PVA can interact with the hydrophilic surface of the modified cellulose, leading to strong hydrogen bonding between the components and creating more paths for ion-coordinating side chains for the ionic transport. The observed high ionic conductivity is driven by local and segmental motions of the polymer chains, which assist the breaking and reforming of the bonds with the cation.[13]

A systematic study of $LiClO_4$-doped PVA/mCellulose composite to understand the ion transport behaviour in polymers, the physical and chemical processes involved in polymer composites are reported here. The Arrhenius model of Vogel–Tammann–Fulcher (VTF) for temperature dependence of ionic conductivity is discussed and correlated the structural changes affected by salt on polymer composite. Attention has been paid on the percolative behaviour of ionic conductivity and correlation of the T_g with activation energy and fragility were studied using Williams–Landel–Ferry (WLF) and VTF equations.

2. Experimental

2.1 *Materials and sample preparation*

PVA was purchased from SDFCL (SD Fine-Chem Limited, Mumbai, India), with molecular weight $M_w \approx 125{,}000$ and its degree of saponification 86–89%. The fibre used in this work was commercial microcrystalline cellulose supplied by Loba Chemie, India; 2-(trifluromethyl) benzoylchloride and pyridine were purchased from Aldrich and are used as received. Initially, calculated amount of cellulose was treated with sodium hydroxide solution at room temperature and stirred for 2 h. Then, the solid obtained was filtered off, and after that, the salt formation was confirmed by solubility test, as it is freely soluble in water. Then the salt was treated with 2-(trifluromethyl) benzoylchloride in the presence of pyridine as a base cum solvent and stirred overnight at 100°C, then dumped into water, the solid obtained (modified cellulose) was filtered off and dried.

The polymer composite films of PVA and modified cellulose are prepared using the solution casting method. Initially, known quantity of PVA and modified cellulose were added in double distilled water with weight ratio of 85 : 15 in different beakers at room temperature and solution was allowed to stir for 36 h for complete dissolution. A different mass fraction of $LiClO_4$ was added to the polymeric solution with continuous stirring for 24 h and the solution was kept aside to get a suitable viscosity. Finally, the obtained viscous solution was poured on to clean glass plate and dried at room temperature. After drying, the films were peeled from the plate and kept in vacuum desiccators for further study. The thicknesses of the prepared films were in the range of 100–150 μm, measured using Mitutoyo-7327 dial thickness gauge of accuracy 0.001 mm. The PVA/mCellulose films doped with different mass fractions of $LiClO_4$ (5, 10, 15, 20 and 25 wt%) were prepared.

2.2 *Characterization*

The prepared PVA/mCellulose doped with different mass fractions of $LiClO_4$ composite films were investigated using Shimadzu Fourier transform infrared (FTIR)-8700 spectrophotometer in the wavenumber range 4000–400 cm^{-1} with the scanning resolution of 4 cm^{-1} and recorded in the transmittance mode. The thermal analysis was carried out using differential scanning calorimetry (DSC Q20) from room temperature to 350°C with a scan rate of 10°C min^{-1} under nitrogen atmosphere. The X-ray diffraction (XRD) measurements were performed using Bruker-D8 advance X-ray diffractometer with Ni-filtered, CuKα radiation of wavelength 1.5406 Å with a graphite monochromator and scan was taken in 2θ diffraction angle in the range from 5 to 50° with a scanning speed of 1 deg min^{-1} and step size of 0.01°. The morphologies of the prepared composite films were examined using JEOL-JSM-6390LV scanning electron microscope (SEM) with resolution of 3 nm specimen holder of diameter 10 mm.

Ionic conductivity of the films was determined at room temperatures using HIOKI-IM3570 impedance analyser. A conductivity cell containing two stainless-steel blocking electrodes with a contact surface area of 1.3 cm^2 was used for the impedance measurement. The measurements at different temperatures were carried out by placing the composite cell in a cryostat with a stability of ± 0.1 K. Precautions were taken in order to measure the impedance data and avoided the signal distortion from reflections by matching the device impedance to the cable impedance. Moreover, explicit force control had been introduced by simply activating an external force loop over existing impedance scheme.

3. Results and discussion

3.1 *FTIR study*

If the two polymers are completely incompatible, each individual polymer does not recognize in infrared spectral terms, the existence due to considerable differences between the infrared spectrum of the composite and the

spectra of the pure components. These differences would be derived from chemical interactions, resulting in the band shifts and broadening. Figure 1 depicts the FTIR analysis of PVA/mCellulose with different mass fractions of $LiClO_4$. In pure PVA/mCellulose composite, a strong band at 3441 and 2920 cm^{-1} corresponds to characteristic stretching vibrations of –OH and C–H groups of both PVA and mCellulose. The IR band for PVA/mCellulose observed at 3441 cm^{-1} has been shifted to 3451 cm^{-1} for $LiClO_4$-doped PVA/mCellulose with decrease in intensity, confirming the formation of intra/intermolecular hydrogen bonding in PVA/mCellulose composites.[14,15]

The 2922 and 2842 cm^{-1} are assigned to aliphatic CH_2 asymmetrical and symmetrical stretching vibrations and the intensity of these bands decreases with the increase of salt concentration. The vibration band at 1734 cm^{-1} corresponds to C–O stretching shifted to 1742 cm^{-1} for 25 wt% $LiClO_4$-doped composite, suggesting that the addition of $LiClO_4$ results in weak interaction between Li^+ ions and the presence of double bonded oxygen groups in PVA/mCellulose matrix. The band that co-exists at 1647 cm^{-1} in pure PVA/mCellulose corresponds to O–H in-plane deformation is shifted to 1655 cm^{-1} with a reduced relative intensity for $LiClO_4$-doped composites, suggesting that the molecular structure of PVA/mCellulose is disturbed by the $LiClO_4$ salt. The vibration at 1639 cm^{-1} corresponds to O–H bending of adsorbed water and vibration at 1620 cm^{-1} is assigned to amide C–O.

The band at 1449 cm^{-1} is attributed to CH_2 wagging of PVA, which is shifted to 1419 cm^{-1} indicating the development of new inter- and intramolecular hydrogen bonds in the polymer matrix. The vibrational band observed at 1337 cm^{-1} are ascribed to CH_2 bending and there is no shift in this band position, but a slight decrease in the intensity is observed. The vibration band at 897 cm^{-1} is assigned to the β-linkage of cellulose. The change in the intensity of ClO_4^- bands appeared between 600 and 650 cm^{-1}, revealing the formation of Li^+ ions. The IR band observed at 628 cm^{-1} is assigned to the 'free' ClO_4^- anion. However, the width of this vibrational band is decreased with the increase of $LiClO_4$ content. These behaviours indicate that there is a limit in the amount of lithium salt that can dissociate in the polymer matrix. All these experimental results suggest that the addition of $LiClO_4$ changes the local chain organization of the polymer matrix.[12]

3.2 *XRD study*

The WAXD patterns of pure PVA/mCellulose and $LiClO_4$-doped PVA/mCellulose composites are shown in figure 2. The figure depicts the crystalline nature of cellulose with an intensive peak at $2\theta = 22.6°$ and amorphous phases of conventional semicrystalline peak between $2\theta = 13–17°$. Even after chemical modification, the cellulose remains as semicrystalline, leading to conclusion that the

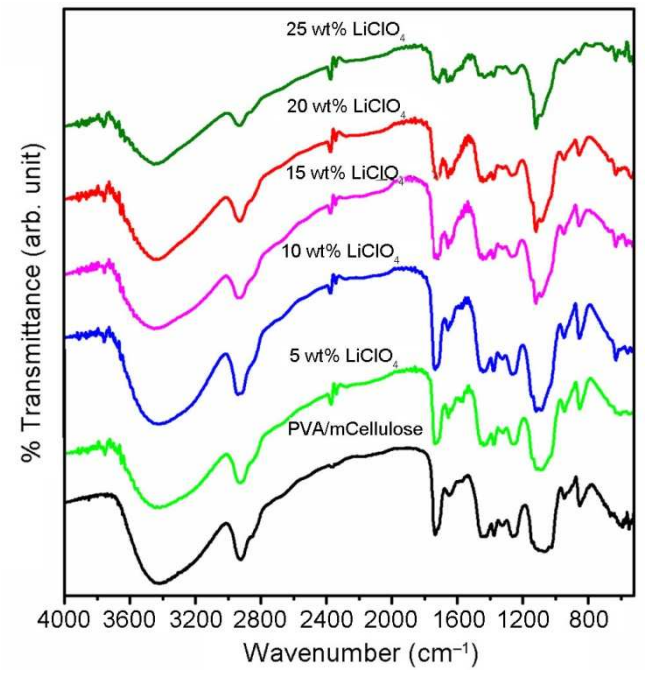

Figure 1. FTIR spectra of pure and different concentrations of $LiClO_4$-doped PVA/mCellulose composite.

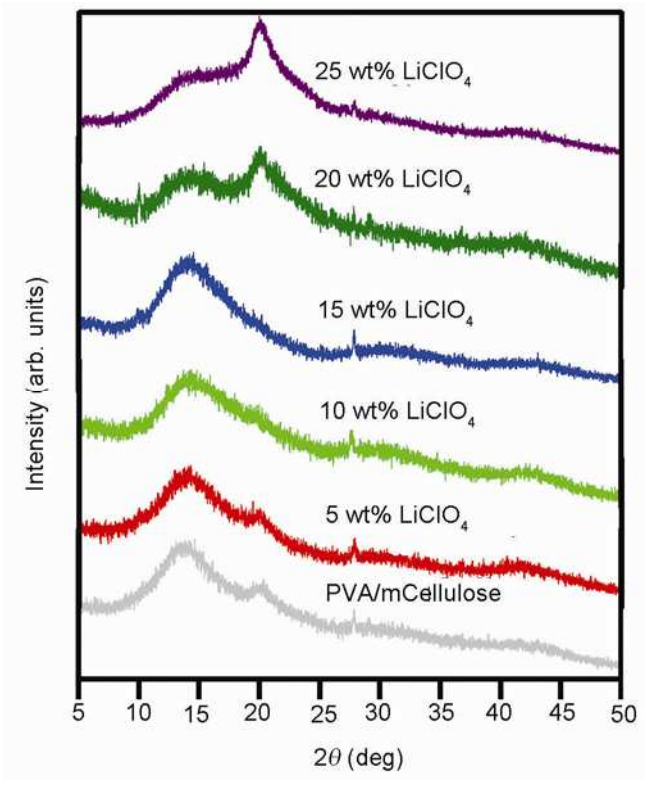

Figure 2. WAXD patterns of pure and $LiClO_4$-doped PVA/mCellulose composite films.

initial crystallinity was retained.[16] The diffraction peak at 13.6° suggests the crystalline nature of cellulose and another peak at $2\theta = 20.5°$ reflects the semicrystalline nature of PVA.[13]

The XRD peaks at $2\theta = 13.6°$ and 20.5° become broaden with the increase in $LiClO_4$ content and also decrease in the intensity, revealing a transformation from semicrystalline to complete amorphous phase. Hence, it can be inferred that the overall morphology and physical properties of the polymer matrix govern the conductivity behaviour.[17] This is another evidence to support the disruption in PVA/mCellulose crystallinity upon complexation with Li^+ ions and the small shoulder at $2\theta = 20.5°$ decreases with the increase in $LiClO_4$ and disappears for 15 wt% $LiClO_4$ content. Diffraction peak at $2\theta = 20.5°$ becomes prominent peak above 15 wt% of $LiClO_4$, revealing that the doping of $LiClO_4$ has no effect on the structural property of PVA/mCellulose matrix and also indicating that the system is not fully amorphous. As Li^+ ions complexes with the polymer matrix, the peaks corresponding to Li^+ ions are not observed, indicating the dissociation of lithium salt in PVA/mCellulose matrix.[16,18,19]

3.3 *SEM analysis*

Figure 3 shows the SEM micrographs of $LiClO_4$-doped PVA/mCellulose polymer composites. The micrographs of both pure as well as $LiClO_4$-doped PVA/mCellulose composite films exhibit a smooth and homogeneous surface with no pores and no interface layer, indicating the complete miscibility and amorphous nature of the prepared composites. Homogeneous distribution of Li^+ ions without any aggregation of $LiClO_4$ particles up to 20 wt% is observed, suggesting that at lower concentration, the lithium particles are well dispersed in PVA/mCellulose matrix. However, above 20 wt% the granule size of lithium particles significantly increased (as shown in figure 3) and some fine streaks and cracks begin to develop on the smooth surface, showing the crystalline structure in the networks. The crystalline nature observed at high salt concentration may be due to salt precipitation as evidenced in XRD analysis.[20,21]

3.4 *DSC studies*

The DSC technique provides information about glass transition (T_g), melting (T_m) and degradation (T_d) temperatures in addition to the associated enthalpy for each process. Figure 4a presents the DSC thermograms of $LiClO_4$-doped PVA/mCellulose composites. For pure PVA/mCellulose, the T_g is observed at 73°C and the T_g of the PVA/mCellulose composites decreased from 73 to 64°C for 25 wt% $LiClO_4$ doping. The gradual decrease in T_g with the addition of $LiClO_4$ confirms the formation of

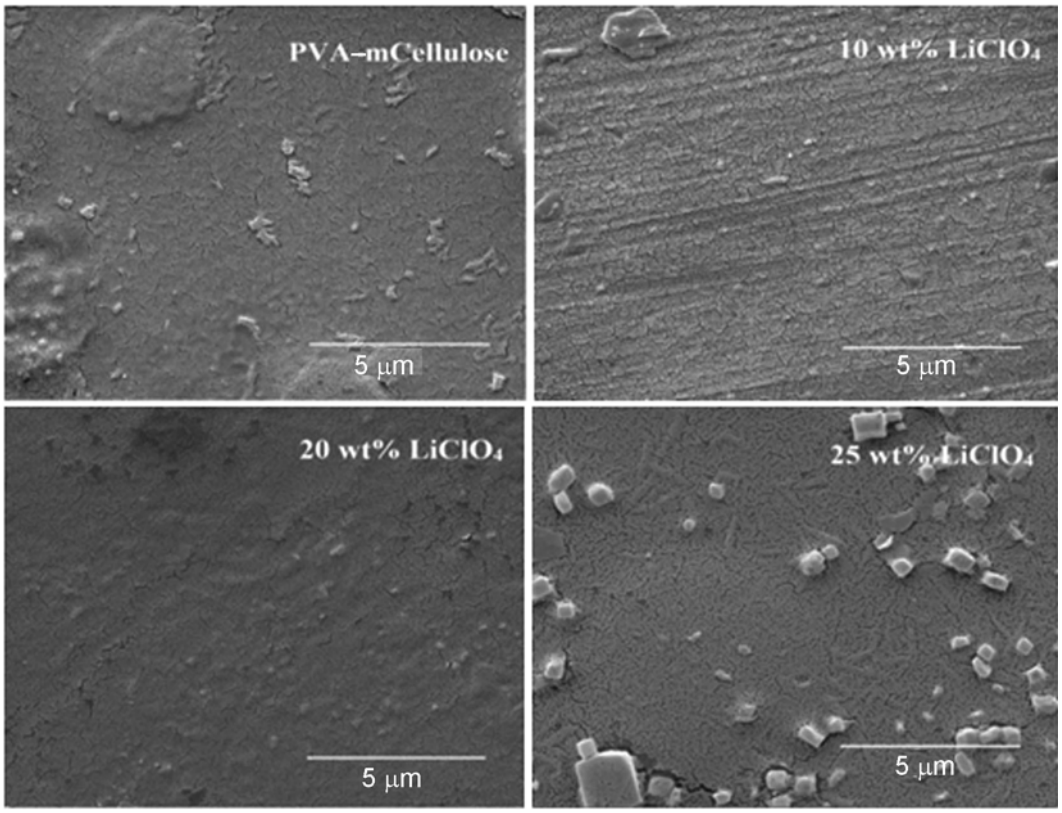

Figure 3. SEM micrographs of pure and $LiClO_4$-doped PVA/mCellulose composite films.

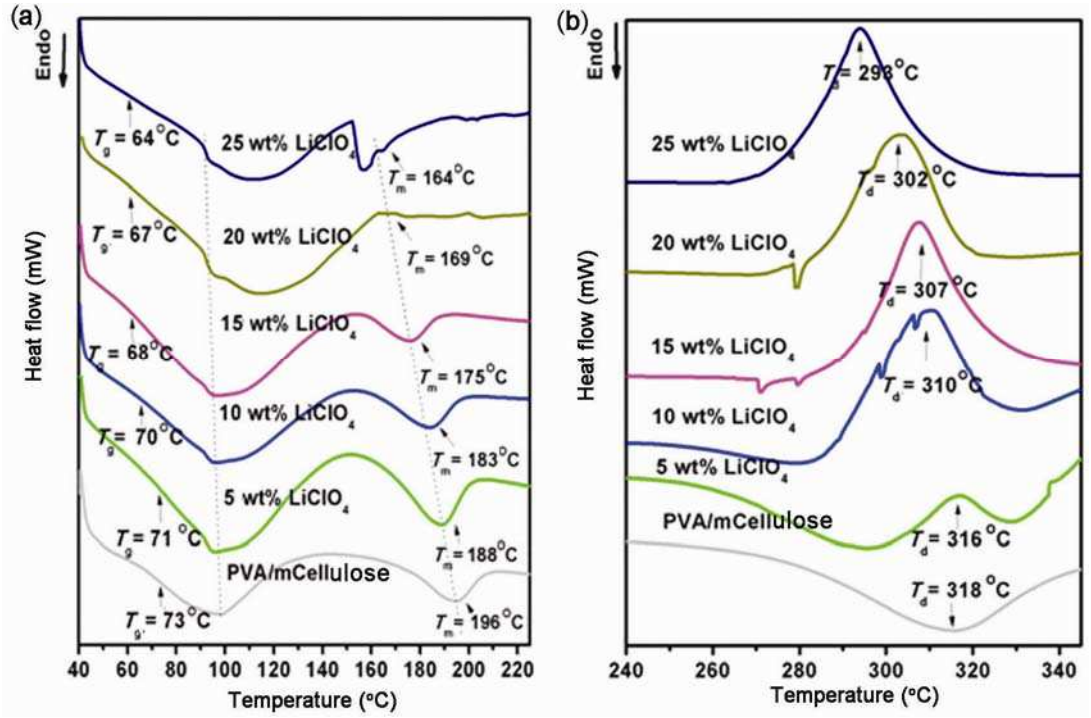

Figure 4. DSC thermograms of pure and $LiClO_4$-doped PVA/mCellulose samples: (**a**) in the temperature of 40–225°C and (**b**) 240–350°C.

complexion between $LiClO_4$ and OH group of the PVA/mCellulose composite.[22] The formation of complexion in the polymer matrix leads to increase in the entropy, results in increase of the segmental movements, leading to reduction in the crystallinity and enhancement in the flexibility of the molecular system.[23]

The T_m of pure PVA/mCellulose is observed at 196°C and decreases with the increase in $LiClO_4$ content within the composite. The depression of the melting point from 196 to 164°C for 25 wt% of $LiClO_4$-doped composites reveals that the presence of large negative value in the thermodynamic interaction parameter and composites are thermodynamically miscible. The T_d of the pure PVA/mCellulose is observed at 305°C and decreases to 293°C with the addition of $LiClO_4$ content, indicating the disappearance of polymer backbone chain, as a result of thermal degradation (as shown in figure 4b). Saturated and unsaturated aldehydes, ketones and the formation of vinyl ester rearranged in the end group are reported as degradation products.

3.5 *Ionic conductivity: percolation (p) at room temperature*

The ionic conductivity is the most important parameter for polymer composites, which has been obtained from the complex impedance plots. Figure 5a presents the percolative behaviour of PVA/mCellulose conductivity as a function of $LiClO_4$ weight fraction. According to classical percolation theory, the conductivity of composite materials increased as conductive filler content was increased. This can be described by a scaling law of the form $\sigma \propto (p - p_c)^t$, where p_c is the percolation threshold and this equation is valid when $p > p_c$ and $(p - p_c)$ is small. As the mass fraction increases beyond the percolation threshold, the conductivity decreases sharply. The exponent t depends on sample dimensionality with calculated values of $t \sim 1.33$ and 2.0 in two and three dimensions, respectively. In our study, the percolation threshold falls in the middle of 15–20 wt%.

The maximum conductivity observed at room temperature is 9.79×10^{-6} S cm^{-1} for 20 wt% of $LiClO_4$ doping, and increase in conductivity is almost gradual with the addition of $LiClO_4$ up to 20 wt%, which attributed to the increase in the number of charge carriers and ionic mobility within the composite. The conductivity decreases beyond 20 wt% due to percolation threshold.[24] Thus, it can be said that either the excess salt did not associate or ions recombine to form neutral ion pairs, thus increases the aggregation results in reduction of free charge carriers and hence the decrease in conductivity beyond 20 wt%. Figure 5b shows the variation of ionic conductivity with reciprocal temperature. The measurement was restricted below 75°C just to avoid any possible dissociation of the sample material. The conductivity of all the composites have increased linearly as the temperature increased. It was assumed that the temperature dependence of the conductivity of the polymer composites follows the

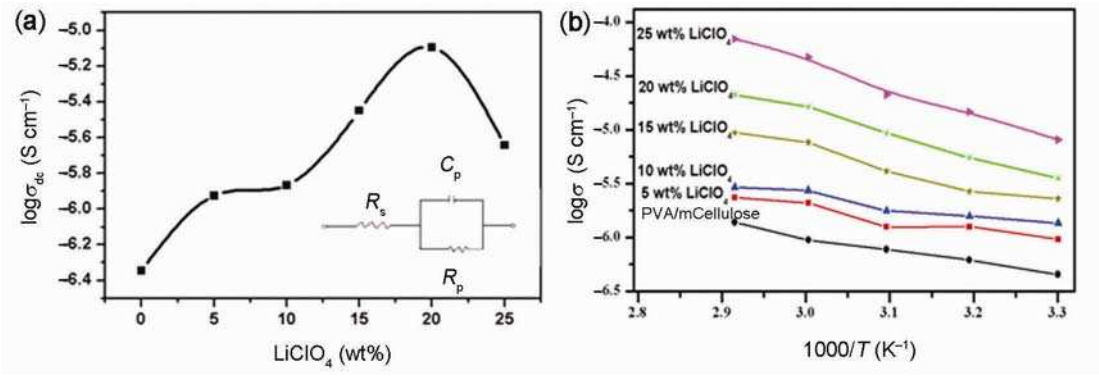

Figure 5. (**a**) Variation of log(σ) as a function of $LiClO_4$ concentration (p) and (**b**) temperature dependence of ionic conductivity of different $LiClO_4$-doped PVA/mCellulose composites.

Arrhenius equation, but the logσ *vs.* 1/T plots of these polymer composites, some observed temperature dependence of logσ *vs.* 1/T, are not linear but polynomial ($n = 2$ or 3), thus, the conductivity of polymer electrolyte are often best fitted by the empirical VTF. For our study, the conductivity of all the composites have increased linearly as the temperature increased. The log σ *vs.* 1/T plot below 323 K temperature follows the Arrhenius behaviour, expressed by

$$\sigma = \sigma_o \exp\left(\frac{-E_a}{k_B T}\right), \tag{1}$$

where σ_o is the dc conductivity of pre-exponential factor, T the absolute temperature, E_a the activation energy and k_B the Boltzmann constant. It is noted that the E_a for pure PVA/mCellulose is 0.149 eV and decreases to 0.128 eV for the highest conducting sample (20 wt% $LiClO_4$), which was calculated using the slope of the plot and Arrhenius equation. This indicates that the ions require lower energy for migration in highly conducting samples,[25] and for the temperature above 323 K the polymer composite exhibits VTF phenomenological relationship

$$\sigma_{dc} = \sigma_o T^{1/2} \exp\left(\frac{B'}{k_B (T - T_o')}\right), \tag{2}$$

where T is the absolute temperature, σ_o the conductivity pre-exponential factor and T_o' the ideal glass transition temperature, i.e., the temperature at which the configurational entropy vanishes, B' the Vogel activation energy related to polymer segmental motion, B' parameter is not an activation energy as the equation clearly shows a non-Arrhenius behaviour at temperatures above T_g. In figure 5b, the solid lines are fits of the VTF equation to the σ_{dc} data and the fitted VTF parameters are summarized in table 1. It is observed that T_o decreases as the salt concentration increases and below T_o the segmental motion freezes. The crossover between Arrhenius and VTF behaviour of σ_{dc} is rationalized by arguing that as VTF dependence is governed by the energy interval ($T - T_o$) and the Arrhenius dependence by the temperature T, for $T \gg T_o$ the two should merge. The VTF model proposes that the ionic conductivity is favoured as a result of the segmental motion of the polymer chain in the polymer matrix. The VTF relation over a wide range of temperature (323–343 K) clearly indicates that a strong coupling exists between the ionic and the polymer chain segmental motions of the $LiClO_4$-doped PVA/mCellulose composite.[26] The approximate temperature at which a crossover from VTF to Arrhenius behaviour or *vice versa* is observed around 323 K and the fitting parameters for VTF and the estimated activation energies for both the Arrhenius and VTF equations are summarized in table 1.

A simple relation of apparent activation energy and correlation between dynamic fragility (f) and T_g for different weight fractions of $LiClO_4$-doped PVA/mCellulose can be achieved from the equivalence of both WLF and VTF equations[3,10,11,19,27]

$$\text{Dynamic fragility } (f) = \frac{C_1^g T_g}{C_2^g} \text{ for } T = T_g, \tag{3}$$

$$\text{Activation energy } (E_g) = \ln 10 R \frac{C_1^g T_g^2}{C_2^g}. \tag{4}$$

Equation (3) suggests that m should be nearly linear in T_g, and $C_1^g = 17.44$ K and $C_2^g = 51.4$ K are the WLF parameters for polymers. Our analysis of the data from equations (3) and (4) shows that for different weight fractions of $LiClO_4$-doped composite exhibit different behaviours in terms of the correlation between m and T_g, there is an approximately linear increase in m with the increase in the T_g, at the same time, another important parameter the apparent activation energy (E_g) at T_g has been investigated. It was found that E_g increases with T_g (shown in figure 6a and b).

Table 1. VTF fitting parameters and fragilities for PVA/mCellulose and $LiClO_4$-doped composites.

$LiClO_4$ (wt%) PVA/mCellulose	E_a (eV) (Arrhenius eqn)	B' (eV) (VTF eqn)	T_g (K)	f	T_o (K)
		0.0148	346	113.9	296.5
5	0.149	0.0149	344	114.9	294.2
10	0.147	0.0150	343	115.3	293.6
15	0.137	0.0152	341	115.9	291.1
20	0.128	0.153	340	116.3	290.4
25	0.142	0.153	337	116.9	287.6

Table 2. Transport parameters of $LiClO_4$-doped PVA/mCellulose composites.

PVA/mCellulose (in wt%)	log σ (S cm^{-1})	E_a (eV)	$\tau \times 10^{-11}$ (s)	n (cm^{-3})	$\mu \times 10^{-10}$ (cm^2 V^{-1} s^{-1})	$D \times 10^{-12}$ (cm^2 s^{-1})	$P(E)$ ($\times 10^{10}$) (s^{-1})
5	–5.926 ± 0.15	0.149	4.82	$2.76 \times 10^{+20}$	1.140	2.98	2.07
10	–5.867 ± 0.14	0.147	4.84	$5.00 \times 10^{+20}$	1.197	3.13	2.06
15	–5.449 ± 0.17	0.137	5.03	$4.07 \times 10^{+20}$	1.693	4.42	1.99
20	–5.095 ± 0.15	0.128	5.19	$1.66 \times 10^{+20}$	2.267	5.92	1.92
25	–5.642 ± 0.17	0.142	4.94	$1.58 \times 10^{+20}$	1.443	3.77	2.02

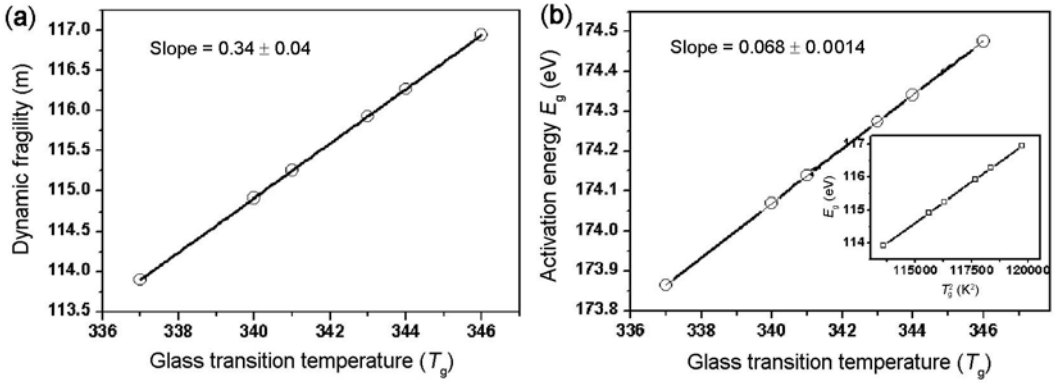

Figure 6. Variation of (**a**) dynamic fragility (m) and (**b**) activation energy (E_g) *vs.* T_g of $LiClO_4$-doped PVA–mCellulose composites.

The quantitative analysis of the increase in conductivity as a function of salt concentration at room temperature is obtained by calculating the activation energy (E_a) using the Rice and Roth model,[28] which states that the conductivity σ can be expressed as

$$\sigma = \frac{2}{3}\left[\frac{(Ze)^2}{kTm}\right] nE_a\tau_o \exp\left(\frac{-E_a}{kT}\right), \quad (5)$$

where Ze, m, k, T, n and τ_o represent the charge of the conducting species, mass of the conducting ions, Boltzmann constant, absolute temperature, number density of ions and time travel of ions between sites. In the present work, the calculation of τ_o (= l/v) was made using l as the hopping distance between two complexation sites and in this work, the short spacing distance between hydroxyl groups in PVA of 2.15 Å[29] and the distance between two repeating units of hydroxyl groups in cellulose of 10 Å[30] and v the velocity of the thermally excited ionic carrier [$v = (2E_a/m)^{1/2}$] was chosen. The other transport parameters such as the ionic mobility ($\mu = \sigma/ne$) and diffusion coefficient ($D = kT\sigma/ne^2$) of the samples have been calculated. Another transport parameter investigated in this work is the number of transitions per unit time $P(E)$, which is expressed as

$$P(E) = \frac{1}{\tau}\exp\left(\frac{-E_a}{kT}\right). \quad (6)$$

The calculated transport parameters for $LiClO_4$-doped PVA/mCellulose composites are listed in table 1. From the table it is clear that, the ionic conductivity increases with the increase in the number density of Li^+ mobile

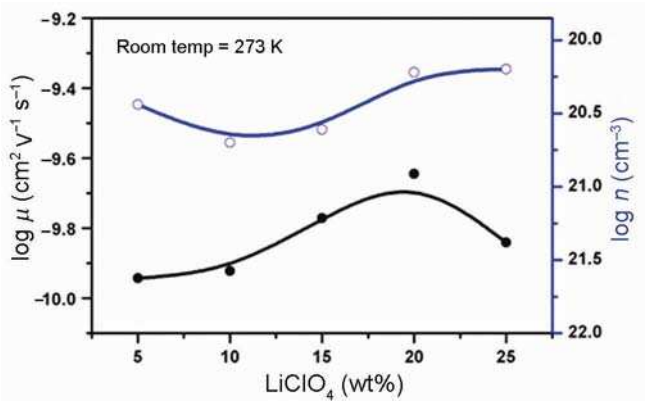

Figure 7. Variation of log μ (•) and log n (○) *vs.* $LiClO_4$ doping concentration in PVA–mCellulose composites.

ions up to 20 wt% doped $LiClO_4$ composites. The values of n, μ and D increased with the increase in the $LiClO_4$ concentration, this is attributed to the availability of more numbers of Li^+ ions for conduction, and beyond 20 wt% $LiClO_4$-doped composites show decrease in n, μ and D value, this is due to the blocking effect created by the $LiClO_4$ in the system. The increase in room temperature conductivity (σ) of $LiClO_4$-doped PVA/mCellulose composite may also be due to the increase in the ionic mobility (μ) and/or increase in Li^+ mobile ion concentration (n) as shown in figure 7 (log μ and log n *vs.* $LiClO_4$ plots).[31] It is known that the ion conducting composites are strongly dependent on ionic mobility (μ) and the mobile ion concentration (n). In order to understand the conduction mechanism in this composite system, it is very essential to estimate the values of μ and n. Hence, to identify the reason for conductivity increase in the present $LiClO_4$-doped composites, a direct determination of ionic mobility (μ) and subsequently, the evaluation of mobile ion concentration (n) have been done as a function of $LiClO_4$.

4. Conclusions

Ionic interactions play an important role in the overall charge transport process in polymer composites. The $LiClO_4$-doped PVA/mCellulose polymer composite has been prepared by the solution casting technique. From the FTIR study, it is confirmed that the strong interactions exist between $LiClO_4$ and PVA/mCellulose composite matrix. The study aimed at improving and extending measurements of conductivity properties in the neighbourhood of the conduction threshold. The maximum ionic conductivity of 9.79×10^{-6} S cm^{-1} is observed for 20 wt% $LiClO_4$ doping at room temperature and variation in conductivity with temperature follows the Arrhenius relation. It has proved that the prepared composites not only show Arrhenius behaviour but also non-Arrhenius behaviour and these studies were discussed in detail. The correlation of dynamic fragility (f) and activation energy (E_g) *vs.* T_g of polymer composites using equivalence of both WLF and VTF equations is also discussed in detail. The calculation of transport parameters like number density of ions and travel time of ions between sites (τ_o), mobility (μ), diffusion coefficient (D) and number of transitions per unit time $P(E)$ reveals the influence of these parameters on the conductivity of polymer composites.

Acknowledgements

We are thankful to Department of Atomic Energy, Board of Research in Nuclear Sciences (BRNS), Government of India, for the research project (2010/37C/7/ BRNS/832) and Department of Science and Technology (DST), Government of India, for the research project (SR/FTP/PS-011/2010). We are also thankful to DST-FIST, Department of Physics, Mangalore University, for providing XRD facility, and to SAIF-STIC, Cochin, for SEM facility.

References

1. Kunthadong P, Molloy R, Worajittiphon P, Leejarkpai T, Kaabbuathong N and Punyodom W 2015 *J. Polym. Environ.* **23** 107
2. Ghaffarian V, Mousavi S M, Bahreini M and Afifi M 2012 *J. Polym. Environ.* **21** 1150
3. Ferry A 1997 *J. Phys. Chem. B* **101** 150
4. Edman L, Doeff M M, Ferry A, Kerr J and De Jonghe L C 2000 *J. Phys. Chem. B* **104** 3476
5. Roth B C, McNerny L K, Jager F W and Torkelson M J 2007 *Macromolecules* **40** 2568
6. Pryamitsyn V and Ganesan V 2010 *Macromolecules* **43** 5851
7. Nigro B, Ambrosetti G, Grimaldi C, Maeder T and Ryser P 2011 *Phys. Rev. B* **83** 064203
8. Sidebottom L D 2000 *Phys. Rev. B* **63** 0234301
9. Hoye S J 2010 *Phys. Rev. E* **81** 061114
10. Soldera A and Grohens Y 2002 *Macromolecules* **35** 722
11. Jin X, Zhang S and Runt J 2003 *Macromolecules* **36** 8033
12. Kesavan, Mathew M C, Rajendran S and Ulaganathan M 2014 *Mater. Sci. Eng. B* **184** 26
13. Bhajantri R F, Ravindrachary V, Harisha A and Crasta V 2006 *Polymer* **47** 3591
14. Macias C E, Bodugoz-senturk H and Muratoglu O K 2013 *Polymer* **54** 724
15. Costa-junior E S, Barbosa-stancioli E F, Mansur A A P, Vasconcelos W L and Mansur H S 2009 *Carbohydr. Polym.* **76** 472
16. Ramesh S, Shanti R and Morris E 2013 *Carbohydr. Polym.* **91** 14
17. Basak P and Manorama V S 2004 *Solid State Ion.* **167** 113

18. Li R, Fei J, Cai Y, Li Y, Feng J and Yao J 2009 *Carbohydr. Polym.* **76** 94
19. Liu D, Sun X, Tian H, Maiti S and Ma Z 2013 *Cellulose* **20** 2981
20. Hashem M, Sharaf S, El-hady M M A and Hebeish A 2013 *Carbohydr. Polym.* **95** 421
21. Hameed N, Xiong R, Salim N V and Guo Q 2013 *Cellulose* **20** 2517
22. Selvakumar M and Bhat D K 2008 *J. Appl. Polym. Sci.* **110** 594
23. Xiao C and Geng N 2009 *Eur. Polym. J.* **45** 1086
24. Planes J, Wolter A, Cheguettine Y, Pron A, Genoud F and Nechtschein M 1998 *Phys. Rev. B* **58** 7774
25. Agrawal R C, Sahu D K, Mahipal Y K and Ashrafi R 2012 *Mater. Chem. Phys.* **139** 410
26. Karmakar A and Ghosh A 2014 *Am. Inst. Phys. Adv.* **4** 087112
27. Zhang S, Painter P C and Runt J 2002 *Macromolecules* **35** 8478
28. Bhargav P B, Mohan V M, Sharma A K and Rao V V R N 2009 *Curr. Appl. Phys.* **9** 165
29. Zhuang P Y, Li Y L, Fan L, Lin J and Hu Q L 2012 *Int. J. Biol. Macromol.* **50** 658
30. Zhi M, Xiang C, Li J, Li M and Wu N 2013 *Nanoscale* **5** 72
31. Chandra A, Bhatt A and Chandra A 2014 *Chin. J. Phys.* **52** 864